Research Square

Preprints are preliminary reports that have not undergone peer review.
They should not be considered conclusive, used to inform clinical practice,
or referenced by the media as validated information.

Antagonistic Activity of Enterobacter mori Pna8 from Pandanus conoideus Against Plant Wilt Pathogens and Its Genomic Characterization

Ahmad Suparmin
ahmad.suparmin@ugm.ac.id
Gadjah Mada University
Lidia Ester Cahyani
PT. Widya Life Science
Ngadiman -
Gadjah Mada University
Hanifrahmawan Sudibyo
Gadjah Mada University
Desy Putri Handayani
Gadjah Mada University
Risky Pasthika Kirana
Gadjah Mada University

Research Article

Keywords: Enterobacter mori, Pandanus conoideus, Biocontrol, Genome sequencing

Posted Date: December 17th, 2025

DOI: https://doi.org/10.21203/rs.3.rs-8204850/v1

License: This work is licensed under a Creative Commons Attribution 4.0 International License.
Read Full License

Additional Declarations: No competing interests reported.

Version of Record: A version of this preprint was published at World Journal of Microbiology and Biotechnology on April 1st, 2026. See the published version at https://doi.org/10.1007/s11274-026-04846-9.

Abstract

This study reports the first isolation of an endophytic bacterium *Enterobacter mori* Pna 8 from *Pandanus conoideus*, a tropical plant whose microbiome has not been previously explored. Strain Pna 8 exhibited strong antagonistic activity, inhibiting *Fusarium odoratissimum* by 55.9% and suppressing *Ralstonia solanacearum* growth, demonstrating dual efficacy against both fungal and bacterial wilt pathogens. Genomic analysis revealed a 4.81 Mb genome containing 4,433 coding sequences enriched in genes associated with carbohydrate metabolism, phytohormone biosynthesis, phosphate solubilization, and stress resilience. Notably, Pna8 lacks pectinolytic CAZymes typical of pathogenic *E. mori* strains, supporting its non-destructive lifestyle. The genome also harbors unique biosynthetic gene clusters, including a lassopeptide absent from pathogenic relatives, and siderophore variants resembling frederiksenibactin. Comparative genomics revealed 119 singleton genes related to transcription, ion transport, and biofilm regulation, highlighting niche-driven evolution and ecological adaptation. Together, these findings indicate that Pna 8 could be further explored as a novel resource for sustainable agriculture and tropical crop protection.

Introduction

Wilt diseases caused by *Fusarium spp.* and *Ralstonia solanacearum* are among the most destructive plant diseases worldwide, severely reducing yields in crops such as banana, tomato, and potato (Dean et al., 2012; Mansfield et al., 2012; Pegg et al., 2019). Foliar symptoms of fusarium wilt include wilting, chlorosis, and vascular discolouration driven by the fungal invasion of the xylem arteries (Gordon, 2017). *Ralstonia solanacearum* impeding water transport via extracellular polysaccharides, consequently creating the swift progression of bacterial wilt (Genin and Denny, 2012). Conventional interventions, including crop rotation and chemical pesticides, are perpetually unsustainable due to the diseases' resilience and persistence (Eljounaidi et al., 2016).

High-throughput sequencing technologies have transformed microbiology by facilitating genomic analyses that reveal the genetic foundations of bacterial traits significant for ecological and agricultural applications (Olanrewaju et al., 2021; Bellotti et al., 2025). Plant-associated bacteria can act as pathogens, resulting in considerable crop losses, or as advantageous symbionts, enhancing plant growth and resilience (Moretti et al., 2021; Wang et al., 2023). Understanding these relationships through genetics is essential for developing ecologically friendly farming practices, such as biocontrol agents for plant diseases.

Enterobacter mori, a bacterium classified as gram-negative and belonging to the Enterobacteriaceae family, plays a dual role in its interactions with plants. Certain strains, such as *E. mori* CX01, is responsible for diseases like mulberry wilt and kiwifruit canker (Zhu et al., 2011; Zhang et al., 2021). Conversely, other strains like *E. mori* AYS9 exhibit traits that promote plant growth and enhance resistance to drought conditions (Fadiji et al., 2023). However, no genomic research has investigated the biocontrol capabilities of E. mori against wilt-causing pathogens.

To date, no studies have been reported on the exploration of endophyte bacteria from the *Pandanus conoideus* plant. Here, we report the first isolation, antagonistic assay and genomic characterization of *Enterobacter mori* Pna8 from *P. conoideus*, a tropical plant native to Southeast Asia and the Pacific. This strain demonstrates strong antagonistic activity against both *Fusarium odoratissimum* and *R. solanacearum* while also carrying plant growth–promoting traits. By combining phenotypic assays with whole-genome sequencing, we reveal unique adaptations including the absence of virulence-associated pectinolytic enzymes and the presence of novel biosynthetic gene clusters, highlighting the biotechnological potential of Pna8 strain for sustainable agriculture.

Methodology

Plant Materials

The *Pandanus conoideus* plant was collected from Sorong, Papua, Indonesia, and subsequently cultivated in pots using regosol. It has been maintained at the microbiological laboratory within the Faculty of Agriculture at Universitas Gadjah Mada Yogyakarta, Indonesia.

Plant wilt pathogenic fungus Fusarium odoratissimum (Fo)

The collection of plant pathogenic fungi was obtained from the Department of Agricultural Microbiology at the Faculty of Agriculture, Universitas Gadjah Mada. The fungal culture was transferred from agar slants and utilized to inoculate the center of sterilized diluted 7X potato dextrose agar (PDA) enriched with yeast. extracted and incubated at 28°C for 7 days.

Plant wilt pathogenic bacteria Ralstonia solanacearum (Rs)

Plant pathogenic bacterium Rs was sourced from the microbial culture collection within the Department of Plant Protection, Faculty of Agriculture, Universitas Gadjah Mada, Indonesia. The bacterial culture obtained from slanted agar was employed to inoculate Casamino-acid Peptone Glucose (CPG) agar, which was then incubated at 37°C for 24 hours. A newly prepared bacterial culture of Rs was introduced into CPG broth and incubated overnight, subsequently harvested via centrifugation at 6. 900 X g at ambient temperature for 5 minutes. The gathered pellets were resuspended in distilled water, and the colony concentrations were adjusted to 10^8 CFU/ml to serve as inoculants for the plant disease treatment assay.

Endophytic bacteria isolation

Endophytic bacteria were isolated from a combination of young, recently emerged leaves sourced from shoot apices and mature leaves obtained from the second and third nodes positioned above the stem base. The leaves were initially rinsed with tap water to eliminate dust and debris, subsequently disinfected, and then processed according to a subtly adapted protocol based on the methodology

described by Araujo et al. (2002). Specifically, the leaves were disinfected by submerging them in 70% ethanol for 1 minute, subsequently immersing them in 2.5% sodium hypochlorite for 3 minutes, and concluding with a submersion in 70% ethanol for 30 seconds, and finally rinsed three times using distilled water. In order to verify the efficacy of the disinfection process, samples of the distilled water from the final rinse were plated onto sterilized 7X nutrient agar, incubated at 28°C for 15 days, and checked for the presence or absence of bacterial colony growth.

The leaves were ground with 5 mL of 0.7% NaCl buffer solution using a sterile mortar and pestle. The resulting tissue extract was incubated at 28°C for 60 minutes to fully release endophytic bacteria. The extract was then diluted in 0.7% NaCl buffer solution, and the dilutions (10^{-1} and 10^{-2}) were plated onto sterilized 7X nutrient agar. The plates were incubated at 28°C for up to 15 days. Bacterial colonies were selected on days 7 and 15 of incubation and identified based on their morphology, including color, size, and shape.

Antagonistic activity of endophytic bacteria against Fo using co-culture method

Fusarium odoratissimum (Fo) was sourced from the fungal culture collection located at microbiology laboratory at Company Widya Life Science, Indonesia. A culture of the fungus was carefully transferred from slanted agar to inoculate the middle of sterilized 7X water diluted potato dextrose agar (PDA) medium enriched with 0. 1% yeast extract (diluted-PDAY). This setup was incubated at a temperature of 28°C for 7 days. Endophytic bacteria were cultivated in a nutritional broth that was maintained at 37°C for 24 hours. Following this, an 8 mm plug of the fungal culture was placed in the center of a fresh diluted-PDAY plate. Each type of endophytic bacteria was inoculated around 25 mm from the edge of the plate using a loop in individual plates. Additionally, control plates with just the fungal plug, which was not inoculated by any bacteria, were created to assess the fungus growth without inhibition. Observations on growth inhibition were made and recorded after 7 and 10 days of incubation at 30°C. The experiment was conducted in triplicate for verification.

Antagonistic activity of endophytic bacteria against Rs using cross streak method

Screening the antimicrobial potential of endophytic bacteria against Rs using the cross-streak method was conducted as follows: Each isolate of endophytic bacteria was streaked horizontally on nutrient agar medium. Following this, the Rs inoculant was cross-streaked horizontally toward each line of endophytic bacteria and incubated at 37°C for 24 hours. The experiment was carried out in triplicate, and the zones of inhibition were measured.

Sequencing and assembly of an endophytic bacterium strain

The endophytic bacterial isolate that demonstrated the strongest antifungal and antibacterial action against Fo and Rs was chosen for molecular identification. The Presto™ Mini gDNA Bacteria Kit (Geneaid, New Taipei City, Taiwan) was used to isolate genomic DNA from overnight cultures of the endophytic bacteria Pna 8 cultivated in nutrient broth. Using a Nanodrop 1000 (Thermo Fisher Scientific) and a Qubit 4 fluorometer (Invitrogen; Thermo Fisher Scientific), the genomic DNA was assessed quantitatively and qualitatively. Sequencing The MGI DNBSEQ G400 technology was used to sequence the genomic DNA, and SPAdes was used to assemble contigs and scaffolds (Prjibelski et al., 2020). CheckM (Parks et al., 2015) and Quast (Gurevich et al., 2013) were used to evaluate the quality of the generated scaffolds. for protein prediction the eggNOG-mapper (Cantalapiedra et al., 2021) and Bakta (Schwengers et al., 2021) were used for protein categorization and functional annotation, respectively. The cluster of orthogonal groups (COG) classifier (v. 1. 0. 5) (Shimoyama, 2022) is one example. The Whole Genome Shotgun project has been submitted to DDBJ/EA/GenBank, where it has been given the accession numberJBKIAY000000000.1.

Comparative genomics

Genomic analyses utilized multiple tools. Average nucleotide identity (ANI) and digital DNA-DNA hybridization (dDDH) were performed with IPGA v1.09 (https://nmdc.cn/ipga/) (accessed on 7 April, 2025) (Liu et al., 2022) and Genome-to-Genome Distance Calculator 3.0 (https://ggdc.dsmz.de/ggdc.php), respectively, to evaluate species relatedness. OrthoVenn3 (https://orthovenn3.bioinfotoolkits.net) (Sun et al., 2023) analyzed shared and strain-specific orthologous clusters. COG annotations enabled functional analysis of gene families. A phylogenomic tree of fifty-six Xanthomonas species was constructed using GTDB-tk v1.4.0 (Chaumeil et al., 2019), and visualized with iTOL (https://itol.embl.de/itol.cgi) (Letunic & Bork, 2019).

The carbohydrate-active enzymes (CAZymes) were annotated with the dbCAN3 Meta Server (automated carbohydrate-active enzyme and substrate annotation) CAZyme annotation database at https://bcb.unl.edu/dbCAN2/ using HMMER and DIAMOND databases, including substrate prediction (Zheng et al., 2023) (accessed 14 May, 2024). Also with Conserved Unique Peptide Patterns (CUPP) online platform (https://cupp.info).

Biosynthetic gene cluster identification

The potential gene cluster of secondary metabolites was determined using the online software antiSMASH 8.0 (https://antismash.secondarymetabolites.org) (accessed on 27 Juni 2025). Clusters were analyzed using the “known clusterblast” module with potential homologs of the MIBiG database entries.

Stastitical analysis

The antagonistic assay was conducted with three replicates. Fungal growth parameters, including distances to the bacterial culture, were analyzed using one-way analysis of variance (ANOVA). Significant differences between treatment means and control were determined using post hoc Tukey's HSD at significance level of $P \leq 0.05$ using R.

Results

Endophytic bacterium isolation and screening for antagonistic activity against Fo and Rs

Endophytic bacteria were isolated from pooled young shoot-tip and mature leaves taken from the second and third nodes above the stem base of *P. conoideus*. A total of five bacterial isolates, designated Pna2, Pna7, Pna8, Pna9, and Pna12, were obtained and analyzed. All isolates exhibited Gram-negative, rod-shaped morphology (**Figure 1A**). Phosphate-solubilizing activity was detected in all isolates except Pna12 (**Figure 1B**). None of the isolates showed evidence of siderophore production (**Figure 1C**).

The antagonistic activity of different endophytic bacteria on Fo growth was measured after 7 and 10 days incubation. The result indicated that all the endophytic bacteria treatment can reduced the fungal pathogen growth (**Figure 2**). Compared to the control (Fo only) which exhibit the largest growth diameter (66 mm). Treatment with Pna 8 reduced the growth diameter of Fo about 50% (29.1 mm) with highest inhibition 63.7% at 7 days after incubation (**Figure 2A and 2B**), followed by Pna 7, Pna 2, Pna 12, and Pna 9 with inhibition of 46.2%, 32.6%, 32.3%, and 20.7%, respectively (**Figure 2A and 2B**). Similar trends were observed after 10 days, where Pna 8 maintained the lowest diameter of growth (43 mm) with percent inhibition slightly decreased to 45.9%. However, the extent inhibition of Pna 7 and Pna 9 sharply declined after 10 days. Therefore, isolate Pna 8 showed the highest inhibition as shown in **Figure 2C** through the incubation time.

The cross-streak assay was used to evaluate the antagonistic characteristics between different endophytic bacterial isolates (Pna 2, Pna 7, Pna 8, Pna 9, and Pna 12) that were streaked horizontally, and the Rs that was streaking vertically (Figure 3). The resulting interaction zones displayed varying degrees of inhibitory effects among the isolates. Notably, Pna 7 and Pna 12 exhibited significant antagonism, as shown by a clear zone of growth inhibition and suppression of the Rs along their confrontation line, indicating the possible release of diffusible antibacterial compounds or competitive exclusion at the point of interaction. Conversely, isolates Pna 2 and Pna 8 showed moderate inhibition, where the growth of the Rs was somewhat limited but continued in close proximity to the bacterial streak. Isolate Pna 12 demonstrated a similar inhibitory effect, evident from a visible decrease in Rs growth near the bacterial streak. Overall, these findings suggest that all examined endophytic isolates hold antagonistic capabilities against the bacterial wilt pathogen. However, the level of inhibition varies by isolate, highlighting differences in their effectiveness as biocontrol agents.

Genome structure and general features

The genome of an endophytic bacterium Pna 8 genome is comprised of single circular chromosome of 4,813,356 bp with 4,433 coding sequences (CDS), the number of contigs 25, N50 values of 767.5 kb, the GC content 55% and 72 tRNA genes (**Figure 4, Table 1**). The origin of replication (OriC) was indicated by a clear display of GC skew transition and terminus. This endophytic bacterium Pna 8 strain encodes diverse pathways for carbohydrate metabolism, including Embden-Meyerhof-Parnas, pentose phosphate, TCA cycle, pyruvate metabolism and galactose metabolism. Based on this genome sequence, suggest that this strain can use D-glucose, D-mannose, L-arabinose, ribose, xylose, L-arabinose.

Table 1. General features of Pna 8 genome

General features of Pna 8 strain Genome	
Genome size (bp)	4,813,356
Number of contigs	25
GC percent	55
N50 (bp)	767,475
Number of CDs	4433
Coding Percentage	90.1
Number of rRNA	4
Number of tRNA	72
Number of tmRNA	1
Number of ncRNA	68
Number of CRISPR	0
Number of sORF	18
Number of OriC	2
Number of OriV	0
Number of OriT	0
Number of gap	0
Completeness (%)/ contamination (%)	99.55/ 0.42
NCBI accession no.	JBKIAY000000000.1

A maximum likelihood phylogenetic tree based on MLST analysis was constructed to determine the genetic placement of Pna 8 within the Enterobacter mori complex (Figure 5). The analysis demonstrated that Pna 8 clustered tightly with E. mori strain ACYC.E9L and positioned a distinct subclade from plant pathogenic strain CX01 and E. mori type strain LMG 25706 as indicated in **Figure 5**. Consistent with the MLST result, the phylogenomic analysis positioned Pna 8 closely related to plant growth promoting *E. mori* strain AYS9 as they grouped together in the same clade with high bootstrap value (**Figure 6A**).

Plant Growth-Promoting (PGP) Activities

Pna8 possesses genes that promote plant growth, including those for phytohormone production, polyamine metabolism, and vitamin biosynthesis **Figure 6B**). Genes for biosynthesis of the phytohormone indole-3-acetic acid (IAA) include aldehyde dehydrogenases (aldA, aldB, aldH), a betaine-aldehyde dehydrogenase homolog (betB), the phenol degradation protein bsdC, aspartate

aminotransferase (aspC), and indole-3-pyruvate decarboxylases (ppdC). The tryptophan biosynthesis genes (trpA, trpB, trpCF, trpD, trpDG, trpE), tryptophan regulators (trpR, trpS), and transporter gene (lysN) suggest that Pna8 can convert indole-3-acetaldehyde to IAA or degrade related aldehydes, supporting the indole-3-pyruvate (IPyA) or indole-3-acetamide (IAM) pathways.

Genes encoding polyamine biosynthesis enzymes, such as lysine/ornithine decarboxylases (ldcC, speA) and agmatinase (speB), produce putrescine from arginine or ornithine. Spermidine synthase (speE) catalyzes the irreversible transfer of a propylamine group from S-adenosylmethioninamine (decarboxy-AdoMet) to putrescine, yielding spermidine. Polyamine uptake and release are facilitated by ABC transporters and permeases (potA, potB, potC, potD, potE, potF, potG, potH, potI). Both polyamine synthesis and transport systems are identified in Pna8.

Folate biosynthesis is indicated by genes encoding GTP cyclohydrolase I (folE), 7,8-dihydro-6-hydroxymethylpterin-pyrophosphokinase (folK), dihydropteroate synthase (folP), folylpolyglutamate synthase (folC), dihydrofolate reductase (folA), and methylenetetrahydrofolate dehydrogenase (folD). Additionally, serine hydroxymethyltransferase (glyA) and tetrahydrofolate aminomethyltransferase (gcvT) support folate-dependent one-carbon metabolism. This complete folate biosynthesis pathway may enable Pna8 to supply folate to P. conoideus, enhancing its growth and stress tolerance.

Pna8 harbors genes involved in phosphate solubilization, including acid phosphatase (aphA), alkaline phosphatase (phoA), phosphate regulon transcriptional regulatory protein (phoB), histidine kinase (phoR), and type II secretion system protein E (gspE). However, nitrogen fixation gene clusters are absent in this strain.

It is worth mentioning that Pna8 encodes a complete pathway for acetoin biosynthesis and catabolism, which contributes to antimicrobial volatile organic compound (VOC) production. Key genes include budB (acetolactate synthase, EC 2.2.1.6), budA (α-acetolactate decarboxylase, EC 4.1.1.5), ilvH and ilvM (acetohydroxyacid synthase subunits), and butA (acetoin reductase/2,3-butanediol dehydrogenase) for synthesis from pyruvate, enabling acetoin and 2,3-butanediol accumulation. Catabolic genes such as acoR (acetoin catabolism regulator), aceF (pyruvate dehydrogenase E2), and lpd (lipoamide dehydrogenase E3) facilitate degradation to acetyl-CoA, maintaining redox balance and conferring resistance to oxidative stress.

KEGG functional categorization

The predicted coding sequences of *E. mori* strain Pna 8 were classified based on function into KEGG categories and compared with the pathogenic strain *E. mori* strain CX01 and the plant growth-promoting strain *E. mori* strain AYS9. Overall, the distribution of annotated genes within KEGG pathways exhibited similarity among the three strains, with most genes being associated with core metabolic functions, cellular processes, and genetic information processing (**Figure 7A**). However, notable differences were observed in categories relating to environmental adaptation, metabolism of cofactors and vitamins, and

signaling pathways, highlighting the lifestyle divergence among the endophytic, pathogenic, and plant growth-promoting strains.

A greater number of genes associated with carbohydrate and amino acid metabolism were found in strain Pna 8, suggesting more metabolic flexibility for utilizing plant-derived substrates within the endophytic niche than in strain CX01. In the same way, the development of pathways for energy metabolism and secondary metabolite biosynthesis can facilitate adaptation to the plant's stable internal environment that is both nutrient-free and stable. In contrast, strain CX01 demonstrated a higher proportion of genes connected to membrane transport and signal transduction pathways, reflecting the necessity for environmental sensing and host interaction during pathogenic colonization.

Notably, strain Pna 8 shared several KEGG characteristics with the growth-promoting strain AYS9, particularly regarding genes involved in cofactors, vitamins, and nucleotide metabolism. These categories are frequently associated with plant–microbe interactions, such as the biosynthesis of vitamin B that can benefit the host plants. However, unlike AYS9, which exhibited significant enrichment in genes related to plant hormone signaling modulation and stress tolerance, strain Pna 8 showed a more evenly distributed profile of pathways, lacking definitive signatures of specialized plant growth promotion. This intermediate profile suggests that although strain Pna 8 may enhance host fitness indirectly through metabolic versatility, it lacks the specialization for growth promotion seen in strain AYS9.

Overall, the KEGG functional annotation indicates that strain Pna 8 possesses a genomic profile tailored for a symbiotic, endophytic lifestyle. It is metabolically prepared for coexistence within plant tissues, with less focus on host manipulation compared to the pathogenic strain CX01, and with diminished specialization in growth-promoting traits compared to strain AYS9. This positions strain Pna 8 as a metabolically versatile yet ecologically distinct endophyte within the *E. mori* species complex.

Carbohydrate and central metabolism

The Pna8 genome harbors a comprehensive suite of genes enabling efficient carbohydrate metabolism, critical for utilizing plant-derived carbon sources in the rhizosphere. Key genes in glycolysis and pentose phosphate pathway link were identified, including glyceraldehyde-3-phosphate dehydrogenase (EC: 1.2.1.12), fructose-1,6-bisphosphate aldolase (EC:4.1.2.13), and glucose-6-phosphate isomerase (EC: 5.3.1.9) also phosphoribosylpyrophosphate synthetase (EC: 2.7.6.1). The capability for starch-derived sugar uptake was indicated form the genes encodes for alpha-glucosidase (EC: 3.2.1.20). Also, beta-glucosidase (EC: 3.2.1.21) the that can metabolize plant-derived cellulosic materials into glucose were identified. In addition, the glyoxylate bypass genes aceA and aceB encoding for isocitrate lyase (EC:4.1.3.1) and malate synthase A (EC:2.3.3.9) which enabling the acetate utilization were also identified.

Comparative analysis of carbohydrate-active enzyme (CAZy) families indicated that Pna 8 displays a generally similar distribution of CAZymes to the strain of CX01 and AYS9, although notable variations in

abundance were apparent among certain families. Pna 8 encoded the largest number of GH and GT families in comparison to CX01 and AYS9, indicating an enhanced repertoire for the processing and modification of carbohydrates (**Figure 7B**). In contrast, CX01 exhibited the most significant proliferation in CE families, whereas AYS9 possessed the largest number of PL-associated genes. For AAs and CBMs, strain Pna 8 possessed marginally fewer representatives compared to both CX01 and AYS9, suggesting a slight decrease in oxidative enzymes and carbohydrate-binding domains.

It is noteworthy, strain Pna 8 lack of pectin-degrading capacity, such as GH28 (7.8%), GH88 (2%), GH74 (2%) and GH94 (2%). While the percentage were found higher in CX01, including 7.8%, 2%, 2% and 2%, for GH28, GH88, GH74 and GH94, respectively. It suggests that Pna 8 avoids damaging host cell walls, consistent with an endophytic, non-destructive role. Overall, despite being the same species, the CAZyme differences highlight niche-driven evolution. This suggests genomic plasticity in *E. mori* adapting to distinct ecological roles.

Survival Mechanisms in the Rhizosphere

Strain Pna8's genome encodes multiple genes that aid survival in the dynamic rhizosphere environment. The chaA, chaB, and chaC2 genes encode a sodium-potassium/proton antiporter and a cation transport regulator, respectively. The ychH gene encodes a stress-induced protein. The rssA and rssB genes encode a patatin-like phospholipase and a two-component system response regulator. Genes involved in the biosynthesis of osmoprotectants (betA, betB) and their transport systems (proX, yehZ) are also present. The soxR and soxS genes, along with pspG, regulate oxidative and envelope stress responses, enhancing resilience against plant-derived reactive oxygen species (ROS) and microbial competition. Exopolysaccharide (EPS) genes (galU, yjbE, gfcC, yjbH) may contribute to biofilm formation. Collectively, these mechanisms enable Pna8 to thrive in the competitive rhizosphere environment.

Fungal cell wall metabolism

Prominently, the gene chbG encodes chitooligosaccharide deacetylase (EC 3.5.1.105), and nagZ encodes beta-N-acetylhexosaminidase (EC 3.2.1.52), which contribute to peptidoglycan recycling by cleaving the terminal beta-1,4-linked N-acetylglucosamine (GlcNAc) from peptide-linked peptidoglycan fragments. This process releases free GlcNAc, anhydro-N-acetylmuramic acid, and anhydro-N-acetylmuramic acid-linked peptides. The exclusive identification of beta-glucanase family GH16 (2.3%, endo-β-1,3(4)-glucanase), chitin-related glycoside hydrolase families GH18 (2.3%), GH19 (1.2%), GH20 (1.2%), and trehalase family GH37 (2.3%) suggests that strain Pna 8 has a unique capability to utilize fungal cell walls as carbon sources or to compete with fungi.

Comparative Genomic Analysis

Comparative genomics analysis between *E. mori* strain Pna8 and *E. mori* strains (AYS9, CX01), *E. roggenkampii* ED5, *E. ludwigii* strain 4b24, *E. kobei* strain ENHKU01, and *Enterobacter* sp. strain J49, conducted via OrthoVenn, revealed 3,478 orthologous gene clusters across the six strains (**Figure 8**).

Strain Pna8 contributed 4,188 orthologous genes, comparable to other *E. mori* strains (4,297 in CX01, 4,114 in AYS9), slightly lower than *E. ludwigii* (4,317), and higher than *E. roggenkampii* (4,004) and *E. kobei* (4,001). This indicates moderate genomic conservation within the genus, with strain Pna8 contributing balanced gene content to the pan-genome.

Strain Pna8 possesses 119 singleton genes unique to this strain across various COG categories. The most abundant was "S" (function unknown, 40 genes, 33.6%), followed by "K" (transcription, 14 genes), "P" (inorganic ion transport and metabolism, 10 genes), and "L" (replication, recombination, and repair, 8 genes) (inset of **Figure 8**). Other categories included "M" (cell wall/membrane biogenesis, 7 genes), "E" (amino acid transport and metabolism, 6 genes), and "T" (signal transduction mechanisms, 5 genes). Mixed categories like "NU" (cell motility/secretion, 3 genes) and "Q" (secondary metabolite biosynthesis, transport, and catabolism, 3 genes) indicate functional diversity. These singletons suggest strain-specific adaptations such as regulatory flexibility (transcription factors in COG K), nutrient scavenging (transporters in COG P), and stress responses (nucleases in COG L). For example, genes encoding fimbrial proteins (COG NU) and methyl-accepting chemotaxis proteins (KEGG ko:K03406) suggest enhanced adhesion and chemotaxis towards plant exudates, while diguanylate phosphodiesterases (COG T, KEGG ko:K21025) and phenolic acid decarboxylases (COG Q, KEGG ko:K13727) hint at biofilm formation and detoxification of plant phenolics.

Strain Pna 8 demonstrated a total of 7 gene family expansions and 212 contractions, revealing a significant net reduction in gene families relative to its pathogenic counterparts (**Figure 9**). In comparison, strain CX01 exhibited 8 expansions and 129 contractions, whereas strain AYS9 exhibited 11 expansions along with 321 contractions. Remarkably, the terminal branch of strain CX01 was marked by an additional significant contraction event entailing the reduction of approximately 100 gene families, emphasizing a lineage-specific phenomenon. the reduction was not observed in conjunction with strain Pna 8 or strain AYS9.

The findings indicate that, although strain Pna 8 possesses a shared phylogenetic origin with pathogens of *E. mori*, its genome has experienced significant contractions, exhibiting fewer expansions. compared to strain CX01 and strain AYS9, the degree of gene family reduction in strain Pna 8 may indicate adaptation processes specific to its ecological niche, which differ from the plant-associated pathogenic existence of *E. mori*.

Biosynthetic gene cluster (BGCs) identification

Based on antiSMASH (version 8.0.2) analysis, the identified secondary metabolite BGCs in strain Pna8 genome and plant pathogenic strain CX01 genome differ slightly. Pna8 has six BGCs compared to five in strain CX01 (**Table 2**). Both strains share conserved BGC types, including azole-containing RiPP, NRP-metallophore/NRPS, terpene-precursor, arylpolyene, and Ni-siderophore clusters. However, Pna8 features an additional lassopeptide BGC absent in strain CX01.

Tabel 2. Comparative BGCs

Feature		E. mori Pna 8		E. mori CX01	
No	Type	Region (From—To)	Predicted Compound (Similarity Confidence)	Region (From-To)	Predicted Compound (Similarity Confidence)
1	Azole-containing-RiPP	1.1 (1,062,814 —1,089,116)	none	1.1 (946,117 —972,419)	none
2	NRP-metallophore	1.2 (1,387,115 —1,440,814)	frederiksenibactin (High)	1.2 (1,277,494 —1,331,606)	enterobactin (High)
3	Terpene-precursor	1.3 (1,624,164 —1,645,063)	none	1.3 (1,516,141 —1,537,040)	none
4	NI-siderophore	13.1 (238,694 —271,122)	aerobactin (Medium)	1.5 (4,392,344 —4,424,772)	aerobactin (Medium)
5	Arylpolyene	15.1 (39,287 —82,871)	arylpolyene (High)	1.4 (2,863,651 —2,907,241)	arylpolyene (High)
6	Lassopeptide	17.1 (35,936 —58,196)	none		
Total BGCs		6		5	

Comparative analysis of the NRP-metallophore/NRPS BGCs in strain Pna8 and the plant-pathogenic strain CX01 strain revealed highly conserved cluster architecture, each spanning approximately 54 kb and classified as type I NRPS systems involved in catecholate siderophore production. Strain Pna8 shows high similarity to the frederiksenibactin cluster (BGC0002413.3 from *Yersinia frederiksenii* ATCC 33641), while strain CX01 matches enterobactin (BGC0002476.2 from *Escherichia coli* K-12 MG1655), a linear oligoester catecholate siderophore and cyclic macrolactone trimer of 2,3-dihydroxybenzoylserine (DHB-Ser). Core biosynthetic genes such as isochorismate synthase (entC-like), 2,3-dihydroxybenzoate-AMP ligase (entE-like), isochorismatase (entB), and 2,3-dihydro-2,3-dihydroxybenzoate dehydrogenase (entA) are conserved in both, alongside NRPS components like amino acid adenylation domains and thioesterases (entH-like) for peptide assembly. Transport-related genes—including TonB-dependent receptors, ABC transporters (fepC/G-like), permeases (fepD), and periplasmic binding proteins (fepB-like) are also shared, facilitating siderophore export and ferric complex uptake. Subtle differences include Pna8's unique mbtH-like protein, potentially enhancing NRPS adenylation efficiency, and a major facilitator superfamily (MFS) transporter absent in strain CX01. Therefore, Pna8 potentially produces distinct structural and functional catecholate siderophore variants.

Although both Pna8 and CX01 strains share conserved core biosynthetic genes for non-ribosomal peptide synthetase (NRPS)-independent siderophore synthetases producing enterobactin, they differ in regulatory elements. Strain Pna8 exhibits a more complex regulatory network, including unique regulators such as ArcA (carbon oxidation repressor), CcpA (catabolite control protein A), and SypG (biofilm formation and host colonization regulator). Shared regulators include ANR (anaerobic transcriptional regulator), FuR variant 1 (ferric uptake regulator), GnfM (nitrogen-fixation regulator), NtrC (nitrogen regulatory protein C), RpoN (nitrogen assimilation and virulence regulator), and ToxT (MSHA biosynthesis regulator). Enhanced ABC-type transporter expression potentially regulated by SypG may support colonization.

Discussion

The isolation and genomic characterization of *E. mori* strain Pna8 from the leaves of *P. conoideus*, an understudied tropical plant native to Southeast Asia and the Pacific, represent a novel contribution to the field of plant-microbe interactions. While *P. conoideus* has been recognized for its nutritional and medicinal properties, its endophytic microbiome remains largely unexplored, with prior studies primarily

focusing on fruit-derived secondary metabolites rather than leaf-associated bacteria (Xia et al., 2018). This study presents the first genomic characterization of *E. mori* strain Pna8, an endophyte from *P. conoideus*. Unlike pathogenic *E. mori* strains such as CX01, which deploy pectinolytic CAZymes to degrade host tissues (Zhu et al., 2011; Zhang et al., 2021), strain Pna8 lacks these virulence factors and instead encodes hydrolytic enzymes (GH16, GH18, GH19) targeting fungal cell walls. This non-destructive strategy underpins its robust antagonism, achieving 55.9% inhibition of *F. odoratissimum* and strong suppression of *R. solanacearum*. Such dual activity positions strain Pna8 as a promising biocontrol agent, similar to *Bacillus* and *Pseudomonas* spp. used in wilt management (Syed Ab Rahman et al., 2018; Bubici et al., 2019).

A key genomic distinction between strain Pna8 and the kiwifruit pathogen strain CX01 lies in their CAZyme profiles and regulatory networks, reflecting divergent evolutionary paths toward mutualism versus pathogenesis. One of the most compelling aspects of Pna8 is its robust antagonistic activity against the wilt pathogens *F. odoratissimum* and *R. solanacearum*. This efficacy is genomically underpinned by specialized genes for fungal cell wall degradation, including chitooligosaccharide deacetylase (chbG) and β-N-acetylhexosaminidase (nagZ), which facilitate peptidoglycan recycling and chitin breakdown mechanisms that enable nutrient competition and direct lysis of fungal hyphae (Veliz et al., 2017; Huang et al., 2022).

Additionally, the complete acetoin biosynthesis pathway (budA, budB) supports volatile organic compound (VOC) production, known to suppress fungal mycelia growth, inducing plants resistance against soil-born pathogen (Gao et al., 2017; Gotor-Vila et al., 2017; Wu et al., 2018). A study reported by Kashyap et al. (2022) shown that acetoin can halted the growth of *R. solanacearum* and also alleviating the plant immune system. In contrast to the pathogenic strain CX01, which relies on pectinolytic for host tissue maceration (Zhang et al., 2021), Pna8 lacks these enzymes, emphasizing a non-destructive, competitive antagonism rather than virulence-driven invasion. These traits echo successful biocontrol endophytes, such as those from date palm tissues that inhibit *Fusarium* via similar hydrolytic enzymes, but strain Pna8's dual efficacy against both fungal and bacterial wilt agents is particularly noteworthy for integrated disease management in crops like banana and tomato (Duraibabu et al., 2022).

The secondary metabolite biosynthetic gene clusters (BGCs) in strain Pna8 unveil untapped antimicrobial potential, with six clusters including a unique lassopeptide BGC suggesting expanded chemical weaponry for biocontrol. The NRP-metallophore/NRPS cluster, resembling frederiksenibactin rather than strain CX01's enterobactin homolog, incorporates mbtH-like enhancers and complex regulators (SypG, ArcA) that may fine-tune siderophore deployment for competition rather than host iron sequestration during infection (Stow et al., 2021). Shared RiPP and terpene-precursor modules, alongside the Ni-siderophore cluster, imply production of broad-spectrum antimicrobials, potentially synergizing with VOCs to disrupt Fo and Rs biofilms. This BGC diversity exceeds that in other *Enterobacter* endophytes, positioning Pna8 as a candidate for metabolite mining, similar to sponge-associated bacteria yielding novel antifungals (Kim et al., 2025). The lassopeptide's novelty, in particular,

could yield cyclic peptides with enhanced stability against plant pathogens, addressing gaps in current biocontrol agents (Rabbee et al., 2024).

Collectively, strain Pna8 exemplifies an underexplored resource in tropical endophytes, with integrated plant growth-promoting and biocontrol traits. Its genomic arsenal suggests potential applications in sustainable agriculture, particularly for managing *Fusarium* and *Ralstonia* wilt diseases where current control methods remain inadequate. Future work should validate these functions in planta and explore metabolite mining from its novel biosynthetic clusters.

Declarations

Acknowledgments

The authors acknowledge Encji Mexica V. P. and Qudwatun Nisaa for preparing the banana plant propagation.

Funding

This work was supported by the Academic Excellence Program C of Universitas Gadjah Mada 431/UN1.P1/KPT/HUKOR/2024.

Author Contributions

AS conceived and designed the experiments. AS and LEC performed experiments. AS, LEC, Ng and DPH analyzed the data. AS, Ng, and DPH interpreted results. AS, LEC, Ng, HRS, HRS, DPH and RPK wrote the manuscript. All authors contributed to the study and approved the final manuscript.

Data Availability

Genomic sequences generated in this study have been submitted to DDBJ/EA/GenBank under the accession number PRJNA1205501 with BioSample ID SAMN46050846.

References

1. Bogas, A. C., Henrique Rodrigues, S., Gonçalves, M. O., De Assis, M., Longo, E., & Paiva De Sousa, C. (2022). Endophytic Microorganisms From the Tropics as Biofactories for the Synthesis of Metal-Based Nanoparticles: Healthcare Applications. Frontiers in Nanotechnology, 4(February), 1–13. https://doi.org/10.3389/fnano.2022.823236
2. Bubici, G., Kaushal, M., Prigigallo, M. I., Cabanás, C. G. L., & Mercado-Blanco, J. (2019). Biological control agents against Fusarium wilt of banana. Frontiers in Microbiology, 10(APR). https://doi.org/10.3389/fmicb.2019.00616
3. Dean, R., Van Kan, J. A. L., Pretorius, Z. A., Hammond-Kosack, K. E., Di Pietro, A., Spanu, P. D., Rudd, J. J., Dickman, M., Kahmann, R., Ellis, J., & Foster, G. D. (2012). The Top 10 fungal pathogens in

molecular plant pathology. Molecular Plant Pathology, 13(4), 414–430. https://doi.org/10.1111/j.1364-3703.2011.00783.x

4. Eljounaidi, K., Lee, S. K., & Bae, H. (2016). Bacterial endophytes as potential biocontrol agents of vascular wilt diseases – Review and future prospects. Biological Control, 103, 62–68. https://doi.org/10.1016/j.biocontrol.2016.07.013
5. Fadiji, A. E., Ayangbenro, A. S., & Babalola, O. O. (2023). Genomic Assessment of Enterobacter mori AYS9: A Potential Plant Growth-Promoting Drought-Resistant Rhizobacteria. Spanish Journal of Soil Science, 13(June), 1–12. https://doi.org/10.3389/sjss.2023.11302
6. Gao, Z., Zhang, B., Liu, H., Han, J., & Zhang, Y. (2017). Identification of endophytic *Bacillus velezensis* ZSY-1 strain and antifungal activity of its volatile compounds against *Alternaria solani* and *Botrytis cinerea*. Biological Control, 105, 27–39. https://doi.org/10.1016/j.biocontrol.2016.11.007
7. Genin, S., & Denny, T. P. (2012). Pathogenomics of the Ralstonia solanacearum Species Complex. Annual Review of Phytopathology, 50(Volume 50, 2012), 67–89. https://doi.org/https://doi.org/10.1146/annurev-phyto-081211-173000
8. Gordon, T. R. (2017). Fusarium oxysporum and the Fusarium Wilt Syndrome. Annual Review of Phytopathology, 55, 23–39. https://doi.org/10.1146/annurev-phyto-080615-095919
9. Gotor-Vila, A., Teixidó, N., Di Francesco, A., Usall, J., Ugolini, L., Torres, R., & Mari, M. (2017). Antifungal effect of volatile organic compounds produced by *Bacillus amyloliquefaciens* CPA-8 against fruit pathogen decays of cherry. Food Microbiology, 64, 219–225. https://doi.org/10.1016/j.fm.2017.01.006
10. Hnamte, L., Vanlallawmzuali, Kumar, A., Yadav, M. K., Zothanpuia, & Singh, P. K. (2024). An updated view of bacterial endophytes as antimicrobial agents against plant and human pathogens. Current Research in Microbial Sciences, 7, 100241. https://doi.org/https://doi.org/10.1016/j.crmicr.2024.100241
11. Huang, Z., Lv, X., Sun, G., Mao, X., Lu, W., Liu, Y., Li, J., Du, G., & Liu, L. (2022). Chitin deacetylase: from molecular structure to practical applications. Systems Microbiology and Biomanufacturing, 2(2), 271–284. https://doi.org/10.1007/s43393-022-00077-9
12. Kashyap, A. S., Manzar, N., Nebapure, S. M., Rajawat, M. V. S., Deo, M. M., Singh, J. P., Kesharwani, A. K., Singh, R. P., Dubey, S. C., & Singh, D. (2022). Unraveling Microbial Volatile Elicitors Using a Transparent Methodology for Induction of Systemic Resistance and Regulation of Antioxidant Genes at Expression Levels in Chili against Bacterial Wilt Disease. Antioxidants, 11(2). https://doi.org/10.3390/antiox11020404
13. Kim, J. A., Choi, S. S., Lim, J. K., & Kim, E. S. (2025). Unlocking marine treasures: isolation and mining strategies of natural products from sponge-associated bacteria. Natural Product Reports, 42(7), 1195–1225. https://doi.org/10.1039/d5np00013k
14. Mansfield, J., Genin, S., Magori, S., Citovsky, V., Sriariyanum, M., Ronald, P., Dow, M. A. X., Verdier, V., Beer, S. V, Machado, M. A., Toth, I. A. N., Salmond, G., Foster, G. D., Lipm, I. P., & Tolosan, F.-C. (2012).

Top 10 plant pathogenic bacteria in molecular plant pathology. 13, 614–629. https://doi.org/10.1111/j.1364-3703.2012.00804.x

15. Moretti, C., Rezzonico, F., Orfei, B., Cortese, C., Moreno-Pérez, A., van den Burg, H. A., Onofri, A., Firrao, G., Ramos, C., Smits, T. H. M., & Buonaurio, R. (2021). Synergistic interaction between the type III secretion system of the endophytic bacterium Pantoea agglomerans DAPP-PG 734 and the virulence of the causal agent of olive knot Pseudomonas savastanoi pv. savastanoi DAPP-PG 722. Molecular Plant Pathology, 22(10), 1209–1225. https://doi.org/10.1111/mpp.13105
16. Olanrewaju, O. S., Ayilara, M. S., Ayangbenro, A. S., & Babalola, O. O. (2021). Genome Mining of Three Plant Growth-Promoting Bacillus Species from Maize Rhizosphere. Applied Biochemistry and Biotechnology, 193(12), 3949–3969. https://doi.org/10.1007/s12010-021-03660-3
17. Pegg, K. G., Coates, L. M., O'Neill, W. T., & Turner, D. W. (2019). The Epidemiology of Fusarium Wilt of Banana. Frontiers in Plant Science, 10(December), 1–19. https://doi.org/10.3389/fpls.2019.01395
18. Rabbee, M. F., Ali, M. S., Islam, M. N., Rahman, M. M., Hasan, M. M., & Baek, K. H. (2024). Endophyte mediated biocontrol mechanisms of phytopathogens in agriculture. Research in Microbiology, 175(8), 104229. https://doi.org/10.1016/j.resmic.2024.104229
19. Sebastianes, F. L. S., de Azevedo, J. L., & Lacava, P. T. (2017). Diversity and Biotechnological Potential of Endophytic Microorganisms Associated with Tropical Mangrove Forests BT- Diversity and Benefits of Microorganisms from the Tropics (J. L. de Azevedo & M. C. Quecine (eds.); pp. 37–56). Springer International Publishing. https://doi.org/10.1007/978-3-319-55804-2_3
20. Stow, P. R., Reitz, Z. L., Johnstone, T. C., & Butler, A. (2021). Genomics-driven discovery of chiral triscatechol siderophores with enantiomeric Fe(iii) coordination. Chemical Science, 12(37), 12485–12493. https://doi.org/10.1039/d1sc03541j
21. Syed Ab Rahman, S. F., Singh, E., Pieterse, C. M. J., & Schenk, P. M. (2018). Emerging microbial biocontrol strategies for plant pathogens. Plant Science, 267(November 2017), 102–111. https://doi.org/10.1016/j.plantsci.2017.11.012
22. Veliz, E. A., Martínez-Hidalgo, P., & Hirsch, A. M. (2017). Chitinase-producing bacteria and their role in biocontrol. AIMS Microbiology, 3(3), 689–705. https://doi.org/10.3934/microbiol.2017.3.689
23. Wang, Y., Sun, Z., Zhao, Q., Yang, X., Li, Y., Zhou, H., Zhao, M., & Zheng, H. (2023). Whole-genome analysis revealed the growth-promoting and biological control mechanism of the endophytic bacterial strain Bacillus halotolerans Q2H2, with strong antagonistic activity in potato plants. Frontiers in Microbiology, 14(January). https://doi.org/10.3389/fmicb.2023.1287921
24. Wu, L., Li, X., Ma, L., Borriss, R., Wu, Z., & Gao, X. (2018). Acetoin and 2,3-butanediol from *Bacillus amyloliquefaciens* induce stomatal closure in *Arabidopsis thaliana* and *Nicotiana benthamiana*. Journal of Experimental Botany, 69(22), 5625–5635. https://doi.org/10.1093/jxb/ery326
25. Xia, N., Schirra, C., Hasselwander, S., Förstermann, U., & Li, H. (2018). Red fruit (*Pandanus conoideus* Lam) oil stimulates nitric oxide production and reduces oxidative stress in endothelial cells. Journal of Functional Foods, 51, 65–74. https://doi.org/https://doi.org/10.1016/j.jff.2018.10.014

26. Zhang, M., Zhang, Y., Han, X., Wang, J., Yang, Y., Ren, B., Xia, M., Li, G., Fang, R., He, H., & Jia, Y. (2021). Whole genome sequencing of *Enterobacter mori*, an emerging pathogen of kiwifruit and the potential genetic adaptation to pathogenic lifestyle. AMB Express, 11(1). https://doi.org/10.1186/s13568-021-01290-w
27. Zhu, B., Lou, M. M., Xie, G. L., Wang, G. F., Zhou, Q., Wang, F., Fang, Y., Su, T., Li, B., & Duan, Y. P. (2011). *Enterobacter mori* sp. nov., associated with bacterial wilt on *morus alba* L. International Journal of Systematic and Evolutionary Microbiology, 61(11), 2769–2774. https://doi.org/10.1099/ijs.0.028613-0

Figures

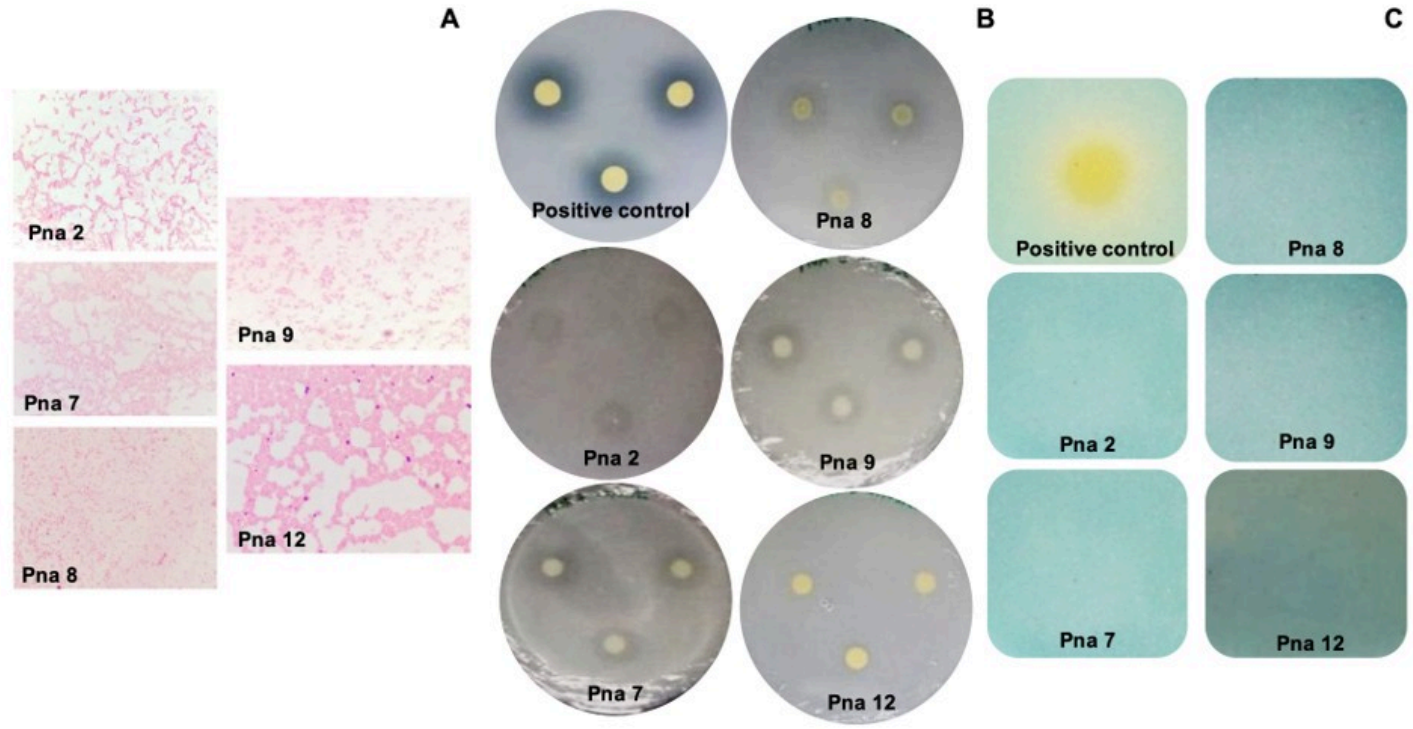

Figure 1

Figure 1

Morphology and plant growth promoting characteristic of the endophytic bacteria isolates. The endophytic bacterial isolates (Pna 2, Pna 7, Pna 8, Pna 9, and Pna 12) were growth on and checked for Gram staining (**A**) phosphate solubilization activity (**B**) and siderophore production (**C**). Assay was conducted with three replicates.

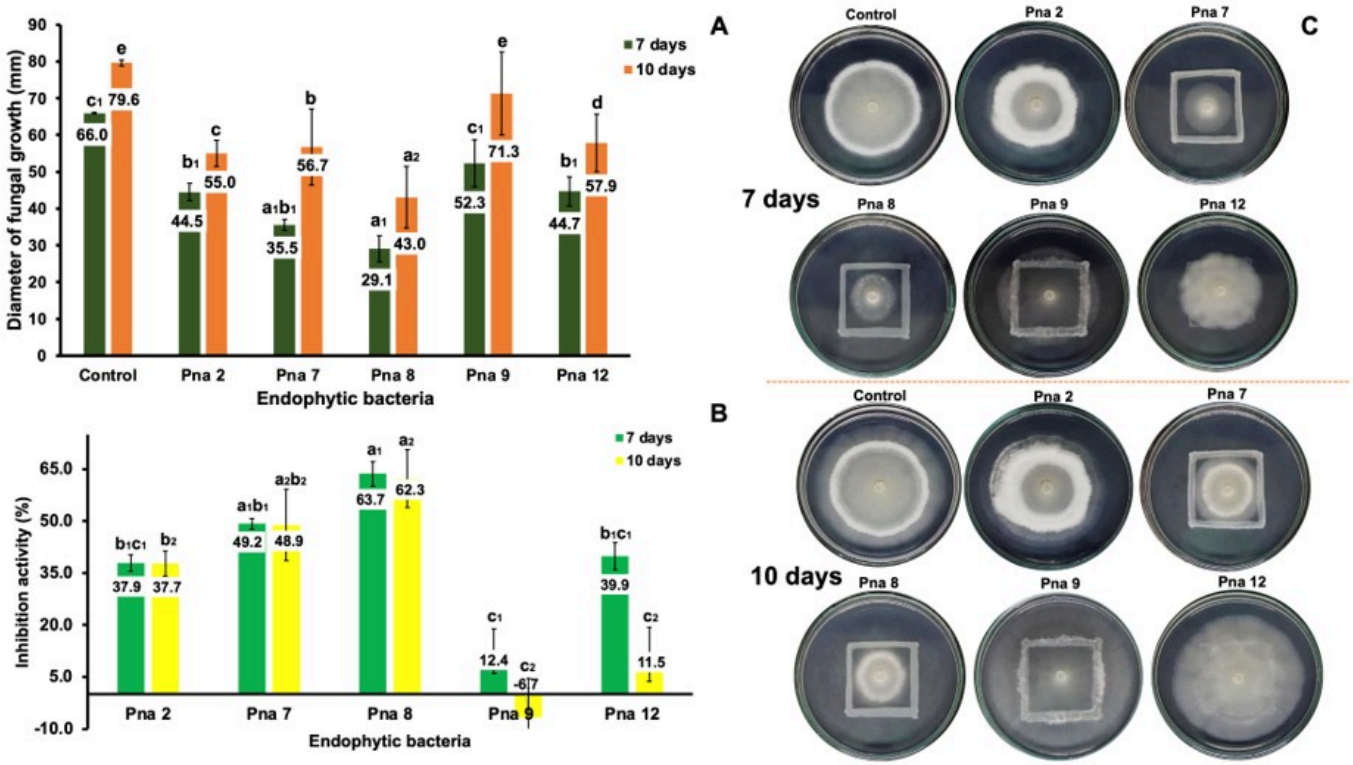

Figure 2

The antagonistic activity of the endophytic bacteria isolates against Fo. The endophytic bacterial isolates (Pna 2, Pna 7, Pna 8, Pna 9, and Pna 12) were growth co-culture with Fo. The growth diameter of Fo (**A**), inhibition activity against the Fo growth (**B**) at 7 days and 10 days incubation. The antagonistic growth between the endophyte isolates and Fo on petridish plate (**C**). Control plates with only the fungal plug without any bacterial inoculation. The test was performed in three replicates. Data are presented as means ± standard deviation. Different letters indicate significant difference ($p < 0.05$) determined by ANOVA followed by Tukey's HSD test.

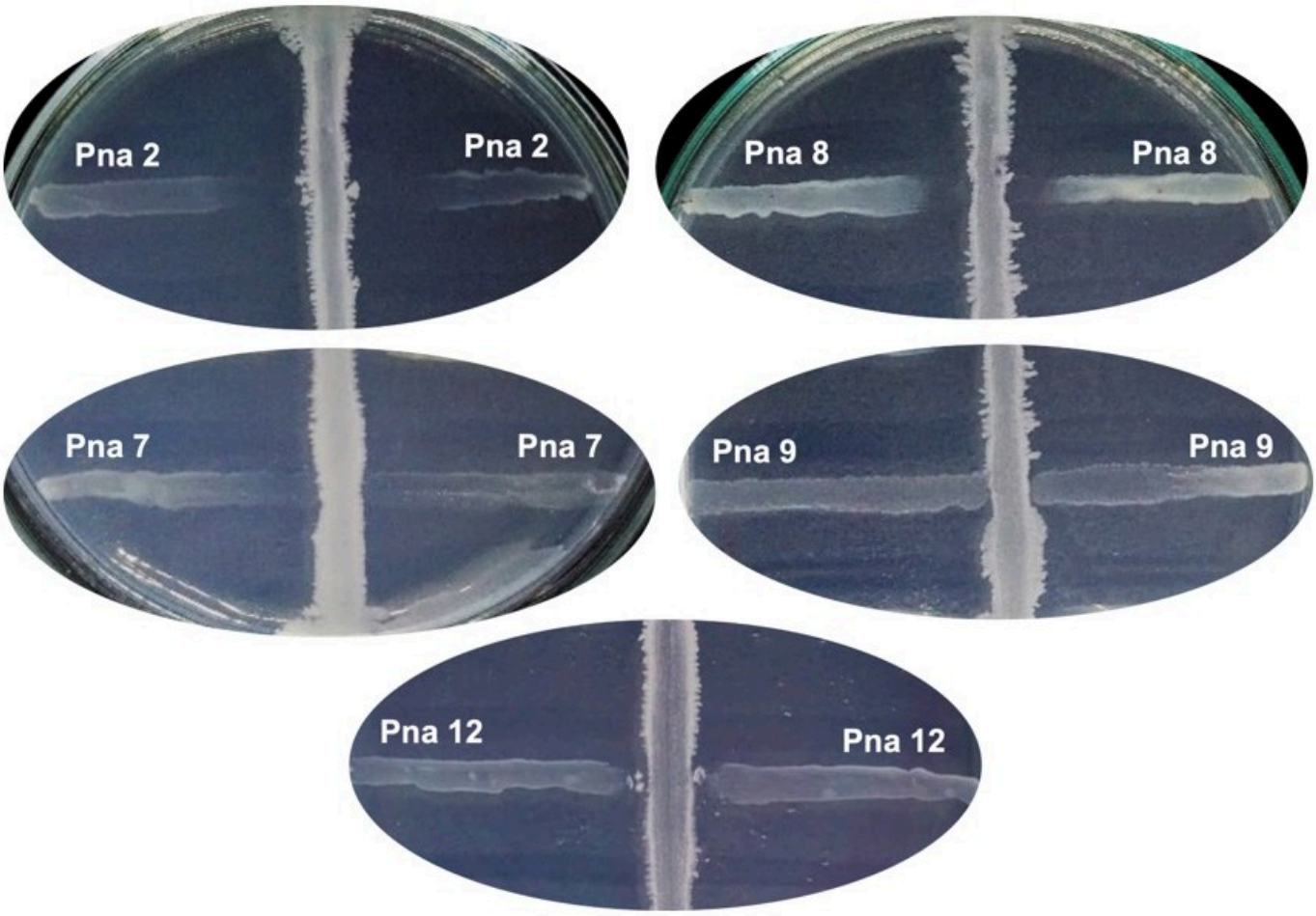

Figure 3

The antagonistic activity of the endophytic bacteria isolates against Rs. The endophytic bacterial isolates (Pna 2, Pna 7, Pna 8, Pna 9, and Pna 12) that were streaked horizontally, and the Rs that was streaking vertically. The antagonistic activity was performed in three replicates.

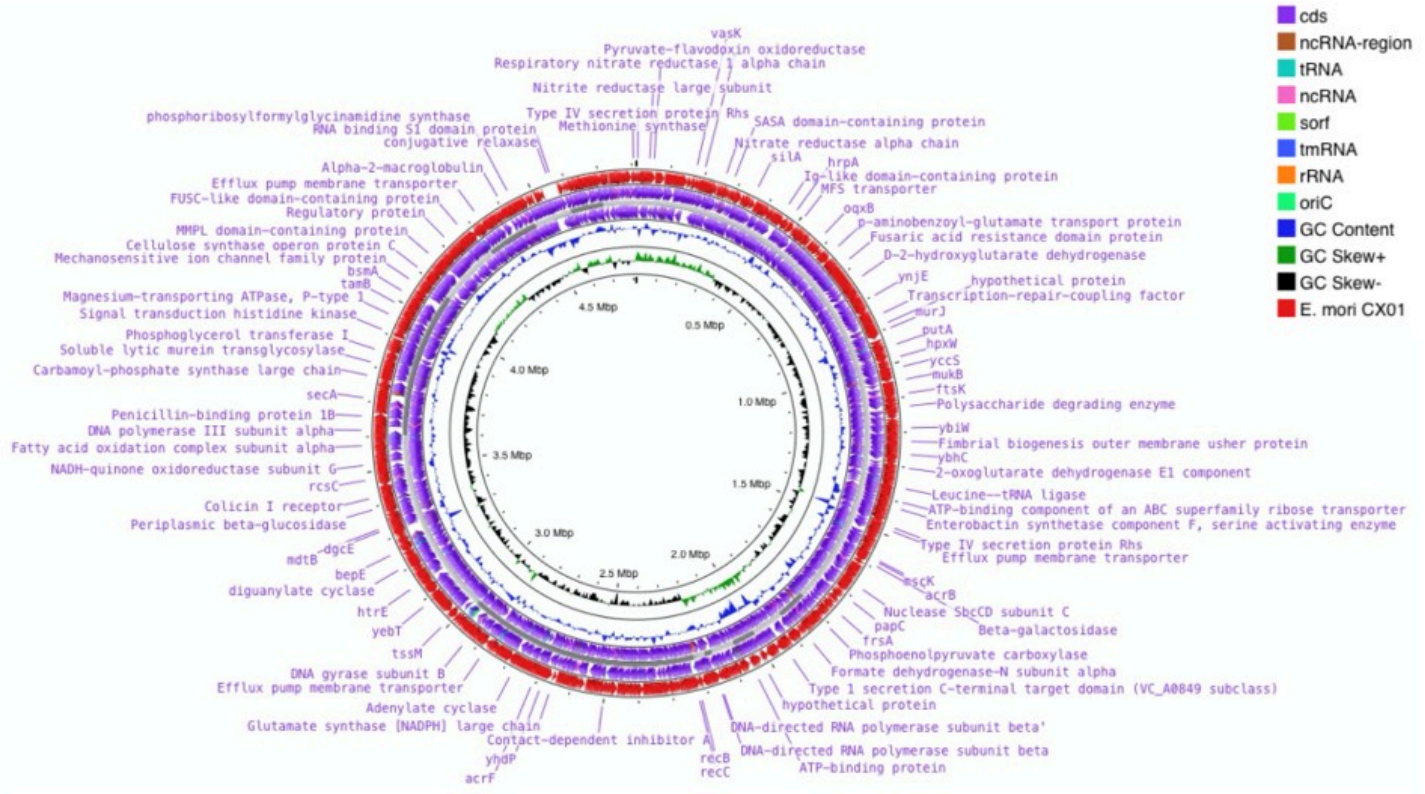

Figure 4

Visualization of the circular genome map Pna 8 strain.

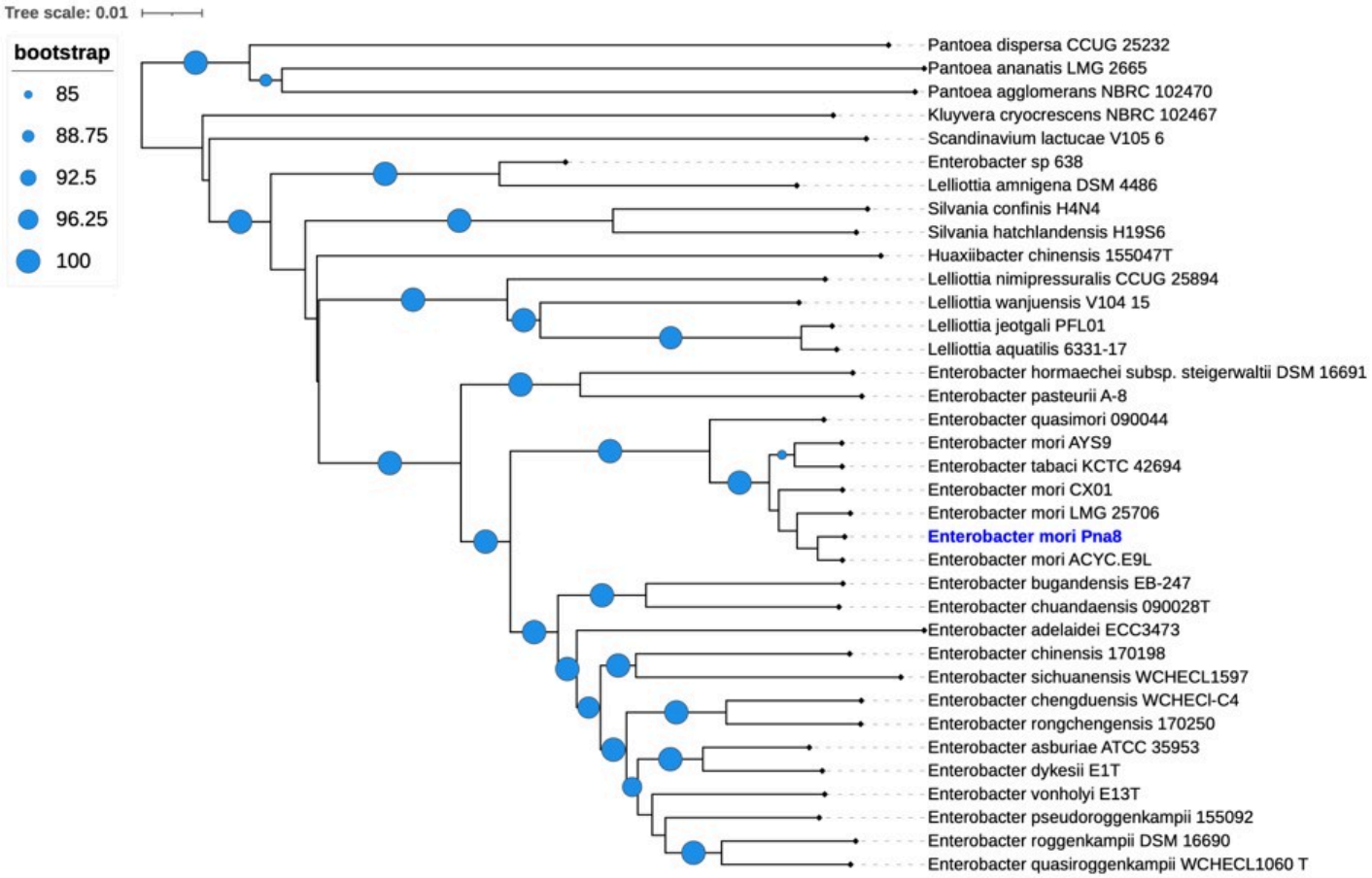

Figure 5

Phylogenetic tree of Pna 8 strain based on the MLST analysis.

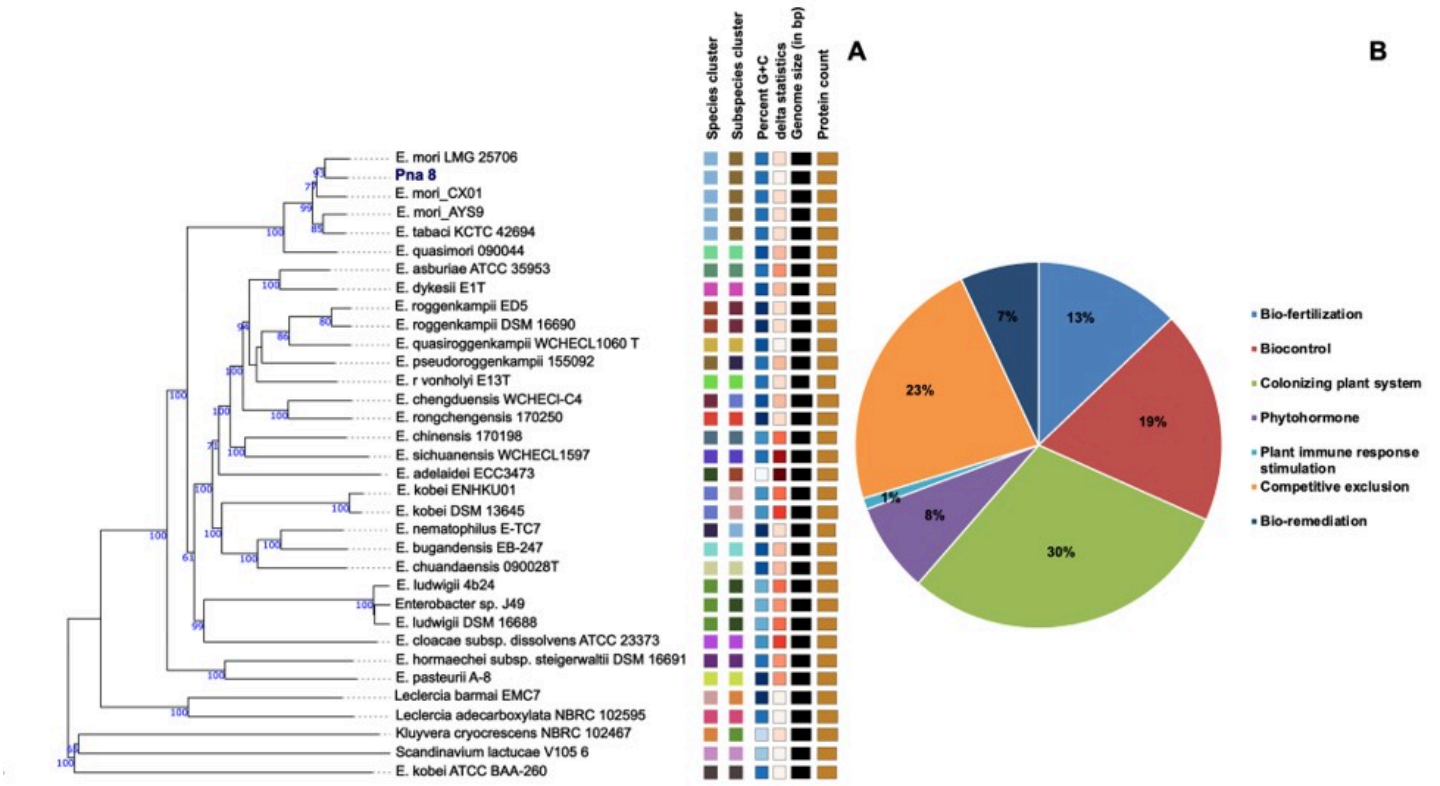

Figure 6

Phylogenomic tree and plant growth promoting genes prediction of Pna 8 strain. Phylogenomic tree (**A**) the genes prediction of Pna 8 that involves in plant growth promoting activity (**B**).

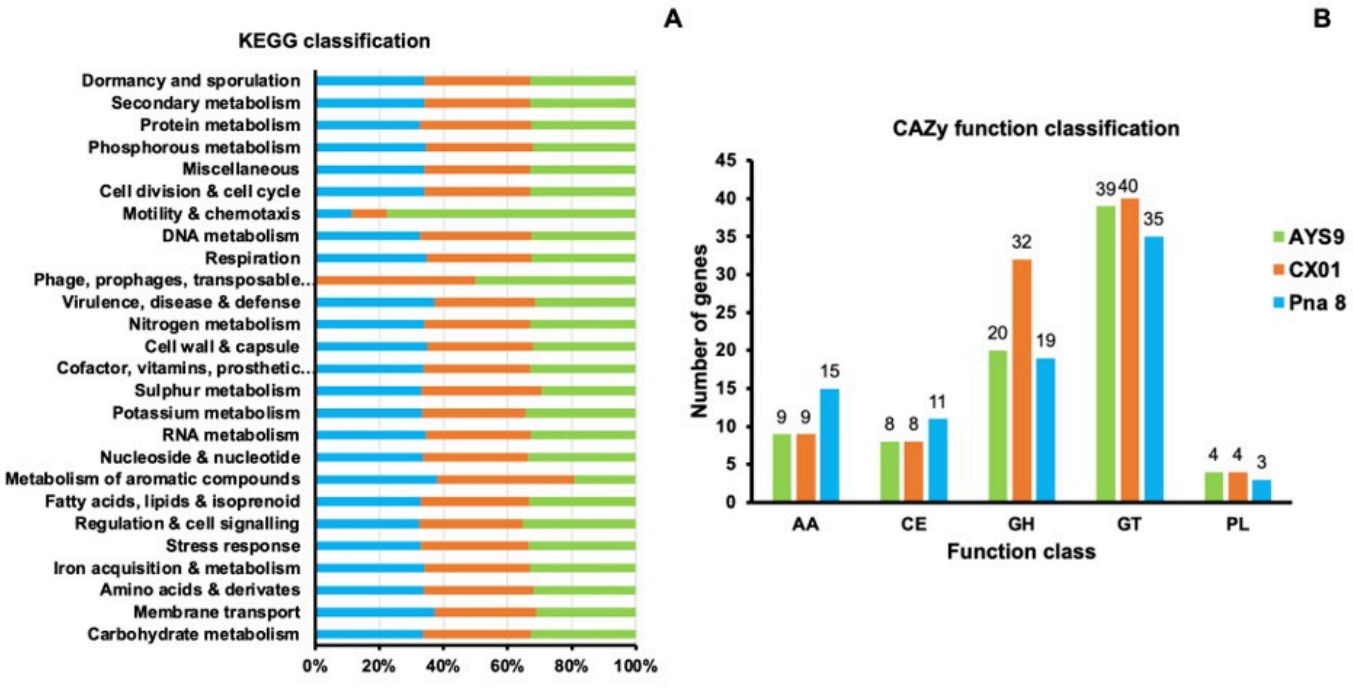

Figure 7

Functional genes prediction. The KEGG classification **(A)** and CAZyme prediction **(B)**

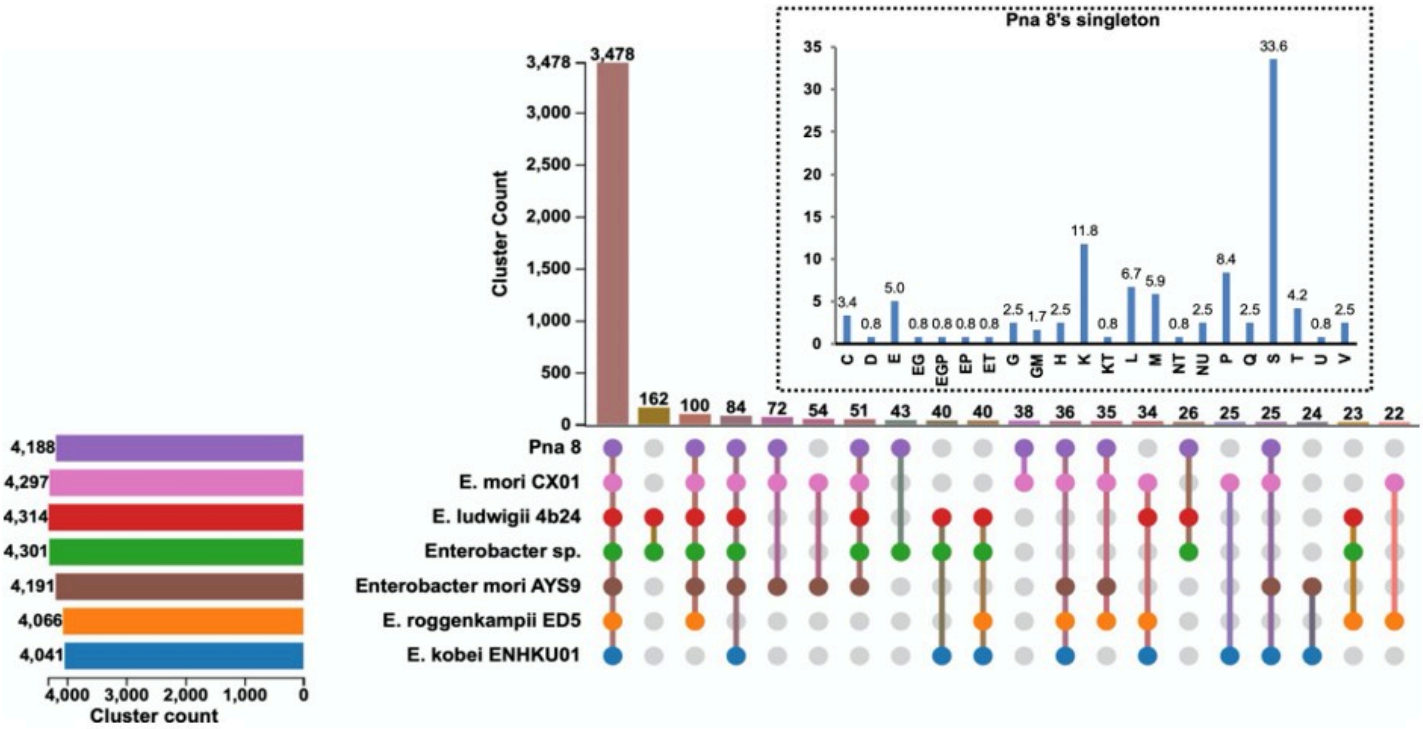

Figure 8

Figure 8

The comparative genomic analysis

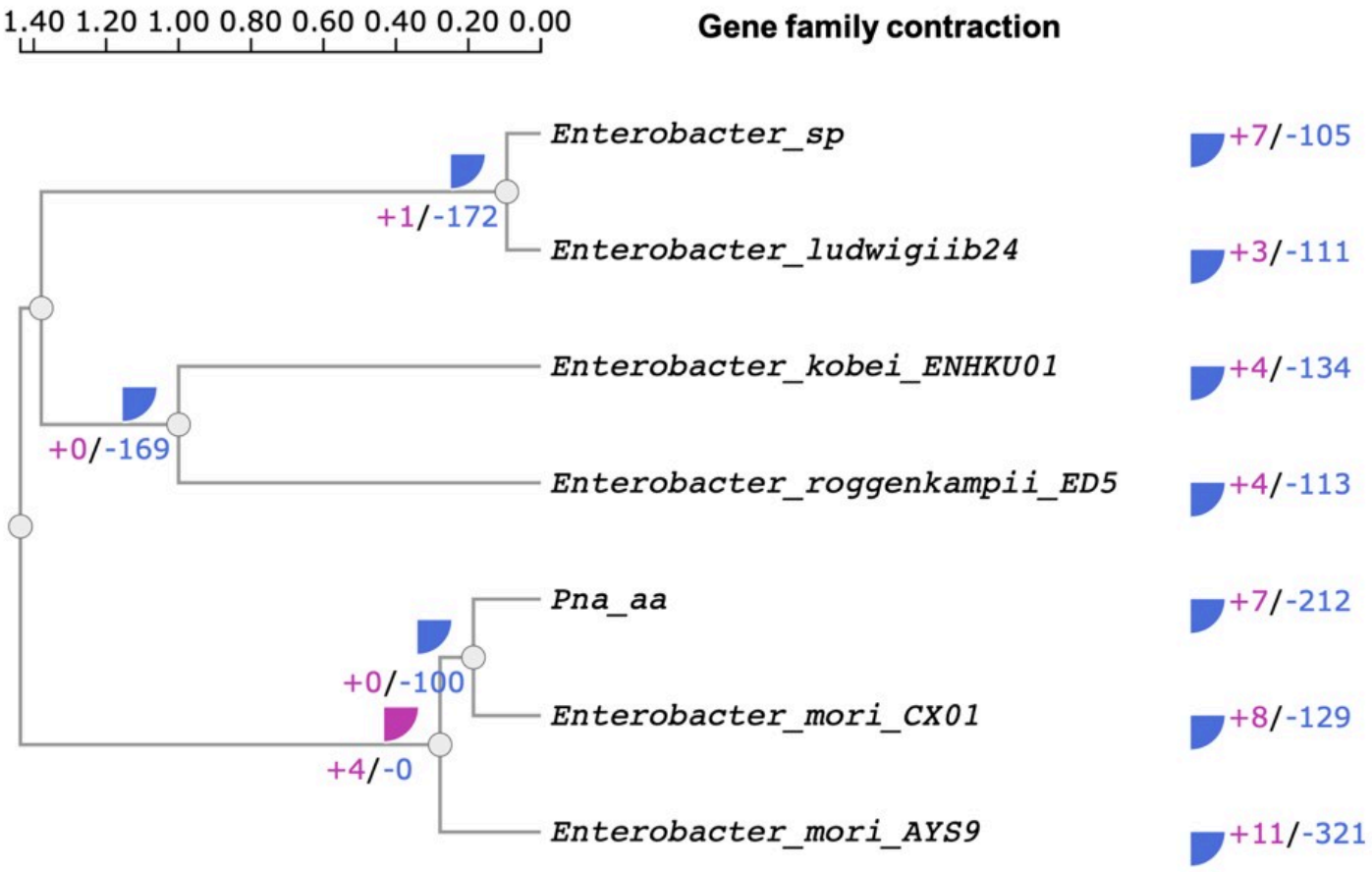

Figure 9

Figure 9

The gene family expansion and contraction analysis